

REVIEW ARTICLE

Conformal microwave array (CMA) applicators for hyperthermia of diffuse chest wall recurrence

PAUL R. STAUFFER¹, PAOLO MACCARINI¹, KAVITHA ARUNACHALAM,
OANA CRACIUNESCU¹, CHRIS DIEDERICH², TITANIA JUANG¹,
FRANCESCA ROSSETTO², JAIME SCHLORFF³, ANDREW MILLIGAN³, JOE HSU²,
PENNY SNEED², & ZELJKO VUJASKOVIC¹

¹Radiation Oncology Department, Duke University, Durham, NC, ²Radiation Oncology Department, University of California San Francisco, San Francisco, CA and ³Bionix Development Corp, Paoli, PA, USA

(Received 4 June 2010; Revised 10 June 2010; Accepted 12 June 2010)

Abstract

Purpose: This article summarises the evolution of microwave array applicators for heating large area chest wall disease as an adjuvant to external beam radiation, systemic chemotherapy, and potentially simultaneous brachytherapy.

Methods: Current devices used for thermotherapy of chest wall recurrence are reviewed. The largest conformal array applicator to date is evaluated in four studies: (1) ability to conform to the torso is demonstrated with a CT scan of a torso phantom and MR scan of the conformal water bolus component on a mastectomy patient; (2) specific absorption rate (SAR) and temperature distributions are calculated with electromagnetic and thermal simulation software for a mastectomy patient; (3) SAR patterns are measured with a scanning SAR probe in liquid muscle phantom for a buried coplanar waveguide CMA; and (4) heating patterns and patient tolerance of CMA applicators are characterised in a clinical pilot study with 13 patients.

Results: CT and MR scans demonstrate excellent conformity of CMA applicators to contoured anatomy. Simulations demonstrate effective control of heating over contoured anatomy. Measurements confirm effective coverage of large treatment areas with no gaps. In 42 hyperthermia treatments, CMA applicators provided well-tolerated effective heating of up to 500 cm² regions, achieving target temperatures of $T_{\min} = 41.4 \pm 0.7^\circ\text{C}$, $T_{90} = 42.1 \pm 0.6^\circ\text{C}$, $T_{\text{ave}} = 42.8 \pm 0.6^\circ\text{C}$, and $T_{\max} = 44.3 \pm 0.8^\circ\text{C}$ as measured in an average of 90 points per treatment.

Conclusion: The CMA applicator is an effective thermal therapy device for heating large-area superficial disease such as diffuse chest wall recurrence. It is able to cover over three times the treatment area of conventional hyperthermia devices while conforming to typical body contours.

Keywords: chest wall recurrence, conformal applicator, microwave array, superficial hyperthermia

Background

Clinical problem

Breast cancer is the most prevalent form of cancer in women, with over 192,000 new cases and 40,000 deaths reported annually in the USA in 2009 [1]. Prognosis is highly dependent upon the location and extent of disease. Despite continued advances in detection and treatment, outcomes for locally advanced breast cancer (LABC) remain dismal with

standard neoadjuvant chemotherapy. Three- and five-year disease-free survival rates are 65% and 55% respectively [2–4]. Inflammatory breast cancer has only 15% five-year survival rate [2]. Failure to control breast cancer at first occurrence dramatically impairs quality of life, with escalating time required for multiple follow-up treatment regimens and increasing chance of complications such as disfiguring ulcerations, oedema, bleeding, and pain requiring narcotics long before death. Recurrence on the chest



Figure 1. Typical cases of chest wall recurrence of breast cancer to be addressed with conformal thermotherapy.

wall occurs in up to 22% of patients following mastectomy, depending on primary size and location, and adjuvant therapy [3]. For those that recur, the median survival following recurrence is just 2 years. As encouraging motivation for the current research, survival ranges from a few months to over 30 years [4], suggesting that significantly improved survival should be possible with improved therapy. To make an impact on this disease, there is an urgent need for adjuvant therapy to increase the duration of local control and improve quality of life for these patients.

Over the past two decades, numerous clinical trials [5–8] including randomised trials in breast and chest wall disease [9–11] have shown that moderate heating to 40°–45°C for 60 min combined with radiation and/or chemotherapy enhances complete response rates and improves quality of life. While encouraging, these results were obtained with equipment that was not optimised for the clinical requirements. The problem remains that hyperthermia devices typically heat only small regions while chest wall disease often spreads over large portions of the torso including the anterior and lateral chest wall and proceeding down the trunk to the abdomen and eventually to the back and shoulders. Typical cases of recurrent chest wall disease are shown in Figure 1. Numerous devices have evolved over the past three decades to heat chest wall disease, including a number of conformal applicators that can heat increasingly larger portions of the torso at one time rather than apply multiple sequential treatments of smaller regions. Following a brief review of devices and techniques available to heat chest wall recurrence of breast cancer, this article focuses on a new heat applicator becoming available for addressing diffuse chest wall disease with a significantly larger treatment area and improved patient interface for more comfortable and convenient thermotherapy.

Current devices for heating chest wall (CW) disease

Methods for heating superficial tissue disease have been reviewed previously [7, 12–14]. While ultrasound (US) systems can be focused precisely to small targets at depth and have shown the ability to smear uniform heating across larger regions of the body [15] even simultaneously with external beam radiotherapy [16–17], most ultrasound systems have difficulty heating contoured anatomy and tissue overlying shallow depth bone. For this reason, treatments of recurrent CW disease are most often performed with microwave sources that limit power deposition to 15–20 mm depth, avoiding discomfort from underlying ribs. While microwave waveguide and horn antennas have been used extensively for treating superficial disease, these bulky applicators are flat and do not conform to the skin surface over typical patient anatomy. In addition, the need for adjustment of power deposition to accommodate variable tissue type, blood perfusion and irregularly shaped disease on contoured anatomy has necessitated a move to multiple antenna systems with variable power deposition. Thus multi-element array devices such as the 15 cm square 915 MHz 4 × 4 planar array microwave system (Microtherm, Labthermics Technologies, Urbana, IL) [18] and 12 cm diameter 8 antenna array (SA-8, BSD Medical, Salt Lake City, UT) [19] have been used to increase the size and adjustability of heating patterns. As applicators increase in size to treat larger areas, the need for flexibility and improved patient interface to handle multiple power connections, surface cooling, and temperature monitoring for treatment control are intensified. The largest surface heating applicators to date include the 25 aperture 915 MHz spiral microstrip array developed at Stanford University, CA [20] and its commercial implementation as a 24 antenna microstrip spiral

array (SA-24, BSD Medical Corp., Salt Lake City UT), the 434MHz flexible PCB microstrip-based contact flexible microstrip applicator (CFMA) [21–23] and the emerging dual concentric conductor (DCC)-based conformal microwave array (CMA) applicator [24–31] which has subsequently been expanded for use with simultaneously administered radiation from either external beam electrons or scanning HDR brachytherapy source [32–35]. This latter applicator is the subject of this article. Many other superficial heating applicators are available, but most are either small area or have large physical size with a patient interface that precludes use for large contoured areas of the torso such as that shown in Figure 1.

Thermometry for monitoring and control of therapy

With appropriate efforts to filter, shield, and align wires perpendicular to the electric field, thermocouples have been used successfully in electromagnetic (EM) fields [36] but are in general not recommended for microwave thermometry [37]. Instead, fibre-optic probes consisting of plastic or glass fibres with non-metallic temperature sensing elements have proven more suitable since they minimise artefacts and field perturbation. Current systems provide essentially artefact-free readout of temperature even in the most intense EM fields, with an accuracy of $\pm 0.3^\circ\text{C}$. The probes are generally inserted through plastic catheters which may be left in the tumour between treatments with good patient tolerance. Following careful multipoint temperature calibration, high resistance lead thermistors exhibit very good accuracy and precision, and long term stability [38]. Similar to fibre-optics, the probes have excellent immunity to electrical readout artefacts and calibration is unique to each sensor so probes are not interchangeable. Even with EMI-immune thermal sensors, careful attention to the size and location of low dielectric constant plastic catheters is required to minimise perturbation of the radiated field in tissue [39]. For monitoring and control of large area heat treatments, a small number of fixed location sensors is generally inadequate to provide feedback to multiple generators for balanced heating across heterogeneous tissues. A common method to improve characterisation of the temperature distribution is to cyclically scan individual sensors through catheters lying on the skin surface and/or implanted at shallow depth in the tumour target. This thermal mapping procedure provides a linear profile of temperature readings at 5–10 mm increments along each catheter, but introduces a delay in reading temperature up to a minute or more while the probe is moving between measurement positions.

While thermal dosimetry for superficial hyperthermia has generally been performed with individual sensors that sample a small number of fixed location points, there are a number of non-invasive approaches under investigation that can quantify more complete 2-D and 3-D temperature distributions. Infrared thermography can be useful in the measurement of large surface temperature distributions, but practical considerations of the hyperthermia applicator blocking direct vision of the heated surface have restricted its usefulness primarily to dosimetry of SAR patterns in split-phantom models [40]. Alternatively, 2D temperature distributions of a surface underlying a hyperthermia applicator may be obtained using a pre-configured thermal monitoring sheet (TMS) fabricated as a uniformly spaced grid of non-perturbing sensors in a thin and flexible sheet. Such a surface-conforming 2D array of sensors has been proposed for clinical monitoring and feedback control of multiple element array microwave applicators when the spacing of sensors corresponds to the spacing of independently controllable heat sources [31, 41, 42]. Other technologies are currently under investigation for their potential to read volumetric temperature distributions deep in tissue. It is well known that MW antennas can be used not only for depositing energy, but also as sensitive receivers to collect temperature-dependent black-body radiation from nearby tissue. Microwave radiometers with multiple frequency bands to interrogate different tissue volumes at depth have demonstrated usefulness in monitoring temperature profiles of tissues up to 50 mm depth [43–47] and for control of microwave hyperthermia [48–50]. Potentially simpler single band radiometers have also been proposed for balancing the power levels of multiple antenna arrays during hyperthermia treatment [30, 51, 52]. While difficulties resulting from tissue movement during scanning remain to be solved, real-time multi-slice magnetic resonance thermal imaging (MRTI) is already a practical technique for non-invasive monitoring of volumetric tissue temperature distributions as well as physiological changes during heat therapy [53–57]. Current efforts with proton resonance frequency shift (PRFS)-based MRTI have demonstrated resolutions on the order of $0.5^\circ\text{--}1^\circ\text{C}$ in 1 cm^3 sensing volumes with less than 1 min scan time for non-invasive monitoring and control of thermal therapy [58–61].

While MR thermal imaging has well-established usefulness for non-invasive volumetric dosimetry of deep hyperthermia in the pelvic region, the impact of MRTI for superficial hyperthermia is unclear at this time – especially for circulating water bolus-coupled applicators located over the thoracic region which is prone to motion artefacts. For the next few years, thermometry to control clinical hyperthermia treatments with large multiple antenna arrays is likely to be

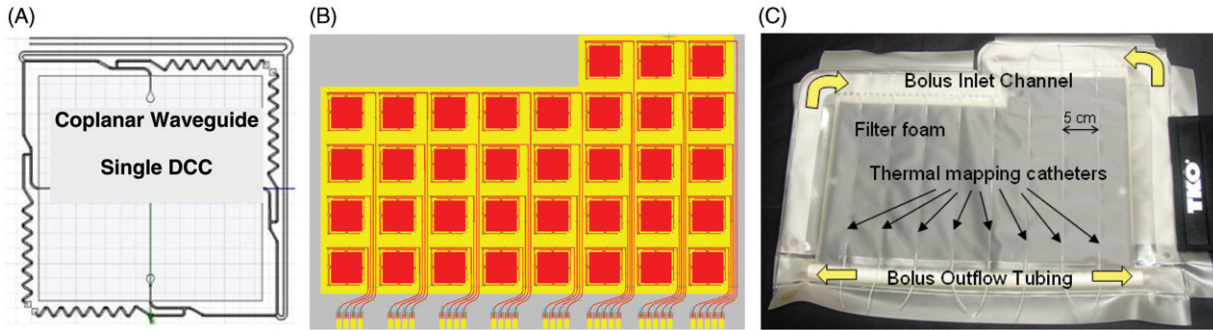


Figure 2. (A) Buried coplanar waveguide feed-line design to excite a single PCB square slot aperture with matching stubs on the fixed-width coplanar slot feeding each excitation port, (B) matched CPW feed-line distribution network to 35 element L-shaped CMA array, and (C) matching 5–10-mm thick water bolus coupling layer with optimised circulation for homogeneous temperature across large surface and integral thermal mapping catheters [34, 35].

accomplished with a single EMI immune sensor located under each antenna, and/or thermal mapping of sensors across the antenna array since those technologies are readily available and provide adequate feedback to control the treatment. For enhanced control of increasingly larger antenna arrays, real-time measurement of tumour temperature distributions should move towards approaches such as 2D thermal monitoring sheets or 3D characterisation of subsurface temperatures with single or multiband radiometers under each independently controllable heat source. These non-invasive monitoring approaches should be implemented soon to provide tighter control of treatment temperatures and higher minimum thermal dose within diffuse superficial disease target volumes.

Conformal microwave array applicator for large area chest wall disease

The CMA applicator is the largest superficial hyperthermia applicator reported to date. It consists of a thin and flexible microwave antenna array, coupled with a surface conforming water-bolus containing circulated temperature-controlled water for skin surface cooling and electromagnetic coupling. An elastic support structure with optional inflatable air bladders holds the entire assembly securely over contoured anatomy. The heating component is fabricated from a flexible printed circuit board (PCB) array of the basic building block element dual concentric conductor (DCC) multi-fed $\lambda/4$ square slot aperture which has been characterised previously and published extensively. Following initial optimisation of the radiation pattern of DCC square slot apertures by Rossetto and others [24–26, 28, 29, 62], Maccarini et al. [63–65] demonstrated the ability to produce similar peripherally enhanced heating patterns that extend out to the perimeter of triangular or other polygon shapes as well as square apertures. Furthermore, the microstrip

feed-lines that distribute power from RF connectors on one edge of the PCB were optimised to include tuning stubs at each DCC aperture feed-point and the original open microstrip design was replaced with a coplanar waveguide buried between two ground planes to reduce losses in the PCB structure and eliminate radiation into air behind the antenna array [66]. These enhancements improved matching and power efficiency of the PCB slot apertures without changing the SAR distribution in tissue.

Figure 2A shows the basic feed-line design of a 3 cm square DCC slot aperture fed via buried coplanar waveguide feed-lines, as optimised with electromagnetic simulations (HFSS, Ansoft, Pittsburg, PA) using a technique that has been reported previously [63–65]. The four tuning stubs match the 50 ohm coplanar waveguide transmission lines to the feed impedance of the DCC slot and provide equal phase and amplitude microwave power to the four symmetric feed-points. The tuning stubs and feed-lines were designed for best impedance match of the DCC apertures radiating into human chest wall tissues through a deionised water bolus. Simulations were performed for a range of typical tissue properties and water bolus thicknesses, and the tuning stubs adjusted to best accommodate an ‘average’ tissue load [63–65]. Figure 2B shows the computer aided design (CAD) layout of a 35 aperture array of 3 cm square DCC apertures intended to fit an L-shaped CMA applicator for heating 42×27 cm area of disease spreading across the upper chest and around the side under the arm to mid back. Figure 2C shows the corresponding water bolus coupling layer that has been optimised for uniform distribution of temperature regulated deionised water to homogenise the temperature across the face of the large array. Following optimisation of the design for fit [67] and uniformity of flow distribution [68], water bolus prototypes such as that shown in Figure 2C have been fabricated by a commercial collaborator (Bionix Development, Paoli, PA). Suitable fabrics with $\sim 2:1$ elasticity have

been formed into a stretchable over-garment vest with adjustable Velcro fasteners to hold the coupling bolus and PCB antenna array securely in place over contoured anatomy. Although there are plans to integrate non-invasive microwave radiometry temperature monitoring into future CMA applicators [30, 51, 69, 70], the current applicator includes an array of skin contacting catheters crossing the water bolus under the centre of each row of DCC apertures for thermal mapping of temperature sensors during treatment. CMA applicators have been fabricated in sizes ranging from 6 to 40 individually powered 2–6 cm square DCC apertures [31, 71, 72]. Custom antenna arrays can be designed rapidly using a commercial CAD program (ADS – Agilent, Santa Rosa, CA) and sent to a PCB manufacturer for fabrication with a 3-week turn-around. Thin water coupling boluses (6–12 mm thick) with quick-connect tube fittings and internal water distribution for uniform circulation of degassed deionised water coolant as in Figure 2C can be fabricated to match the size and shape of the custom arrays.

Results

Over the past decade, the CMA applicator design has evolved in terms of antenna construction, water

bolus shape and internal water distribution, and outer elastic support structure. These changes have all contributed to an improved patient interface that accommodates an increasing range of size and shape of disease over highly contoured anatomy without significant change in the SAR pattern of the basic DCC-based CMA applicator. The following sections briefly summarise the results of four evaluations of CMA applicator performance in terms of: (1) conformity of current CMA applicator design to contoured anatomy, (2) theoretical ability of current CMA to heat tissue uniformly over contoured anatomy, (3) SAR measurements of the most recent buried coplanar waveguide printed circuit array configuration, and (4) a clinical evaluation of heating performance of microstrip based CMA applicators in 13 chest wall recurrence patients.

Performance evaluation of CMA applicators – conformity to chest wall

The ability of CMA applicators to conform to typical patient contours was assessed in both torso shaped phantom models that could be scanned with standard computerised tomography (CT) and in an IRB approved volunteer study to assess comfort and secure fit of the recently optimised conformal water bolus vest with serial MR imaging. Figure 3A shows

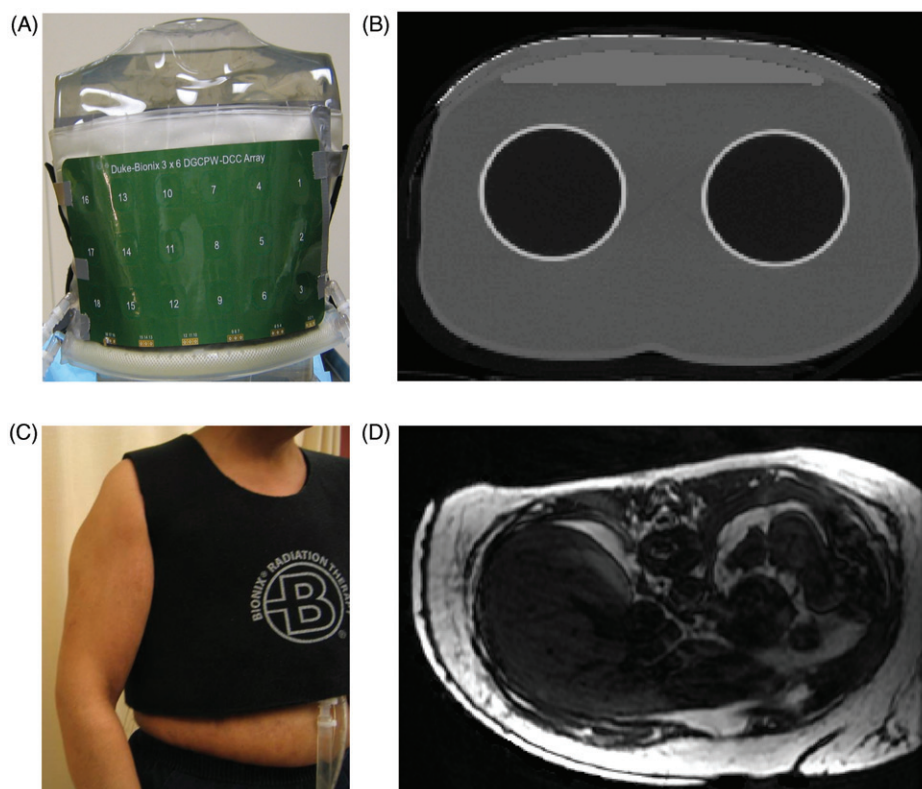


Figure 3. CMA applicator conformity to contoured chest wall: (A) Photo of 18-element DCC array coupled with 9-mm thick water bolus to torso phantom, (B) CT scan cross section of torso phantom through one row of the 18 element DCC array, (C) Elastic outer support vest, (D) MR scan showing conformal water bolus on a mastectomy patient.

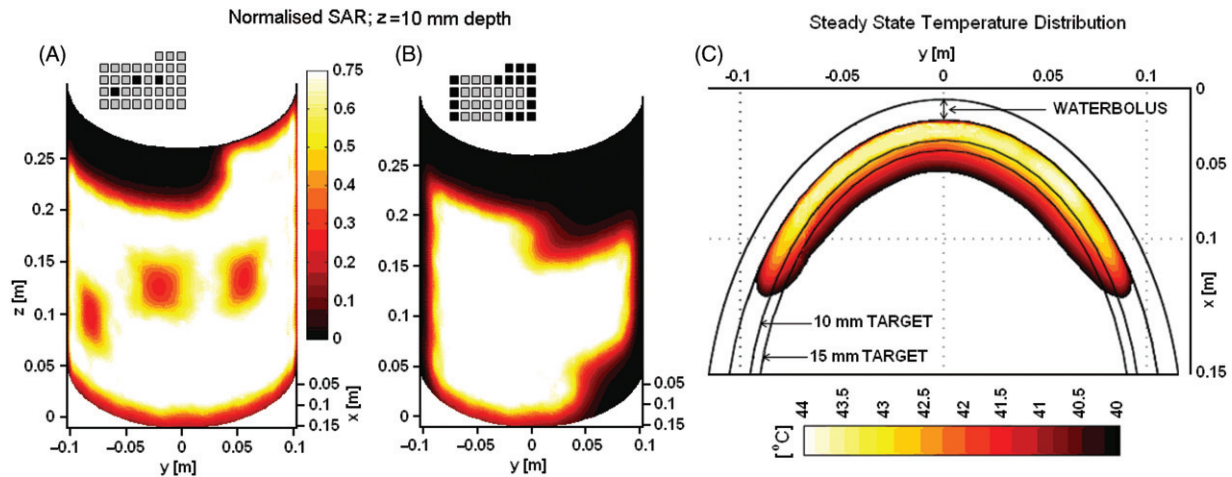


Figure 4. Simulated SAR and heating pattern on contoured surface of an elliptical tissue model. (A) Normalised SAR 10 mm deep in muscle for a 35 element CMA with three centrally located DCC antennas powered off to demonstrate localisation and control of heating; (B) Normalised SAR pattern 10 mm deep in muscle on the contoured torso for a second power configuration as shown inset (selected peripheral apertures in black turned off). (C) Steady-state temperature distribution inside the simulated target volume extending 15 mm deep, as calculated for the SAR distribution of Figure 4B.

an 18-element coplanar waveguide array wrapped around the chest wall region of a torso model overlying a surface-conforming rectangular water bolus (Bionix Development, Paoli, PA). The applicator was secured around the contoured surface with a vest shaped elastic over-garment such as that shown in Figure 3B. A CT scan of the torso model is shown in Figure 3C to demonstrate the ability of CMA applicators to conform to an appropriately contoured surface with no trapped air pockets. The thin broken white line along the top of the 9-mm thick water bolus is the copper DCC array apertures. Figure 3D demonstrates the close conformal fit of the water bolus vest to a mastectomy patient chest wall. In this image, the outer white region extending from the sternum under the arm to the back is a 6-mm thick water bolus separated from the skin by 0.5 mm PVC. The air filled catheters for thermal mapping of tumour target surface temperatures are seen (black) in intimate contact with skin (black) and water bolus (white). Results of the 10-patient study of comfort and secure fit for a 90-min treatment interval will be reported separately.

SAR and thermal simulations for large area disease

Thermal therapy for chest wall disease is challenging due to the large and highly contoured surface areas to be treated. It typically requires multiple treatment fields with standard 100–430 cm² superficial hyperthermia applicators found in most hyperthermia clinics. Larger conformal applicators that can accommodate contoured anatomy are preferred. Several multiple element array applicators have been reported in the literature, but have not been

characterised for heating properties over contoured anatomy. For this effort, electromagnetic (EM) and thermal simulations were performed using commercial software and 3D simulation approaches that have been described previously for EM [63, 64, 66] and thermal [34, 35, 68, 72] modelling of planar applicators. EM simulations were performed with HFSS (Ansoft) for a 42 × 27 cm L-shaped CMA to assess the ability to deliver localised heating to diffuse chest wall disease that extends from the sternum over a mastectomy scar and around the side to the back. The computer model for this situation consisted of a 15 mm deep tissue target along the contoured surface of an elliptical shape muscle-equivalent phantom ‘torso’ coupled to the DCC array with a 9-mm thick deionised water bolus. The iso-SAR patterns 10 mm deep in tissue shown in Figures 4A and 4B demonstrate the ability of a 35-element CMA to deliver adjustable heating patterns over a large contoured surface with no unintended gaps in effective coverage <50% SAR_{max} within the array perimeter. Heating was further characterised using finite element simulation software, Comsol (Stockholm, Sweden) to calculate the predicted temperature distribution for the array configuration of Figure 4B. Shown in Figure 4C is the steady-state temperature distribution in one cross-sectional plane of the heating array for a 42°C water bolus. Blood perfusion rates of 2 and 1 kg/m³/s were assumed inside the target and surrounding muscle tissue for the tissue properties reported in Maccarini et al. [66]. The temperature distribution in Figure 4C shows thermal elevation into the hyperthermic temperature range (40–44°C) everywhere within the 15 mm deep target tissue under the perimeter of the active heating elements.

Int J Hyperthermia Downloaded from informahealthcare.com by Duke University Medical Center Library on 09/27/10 For personal use only.

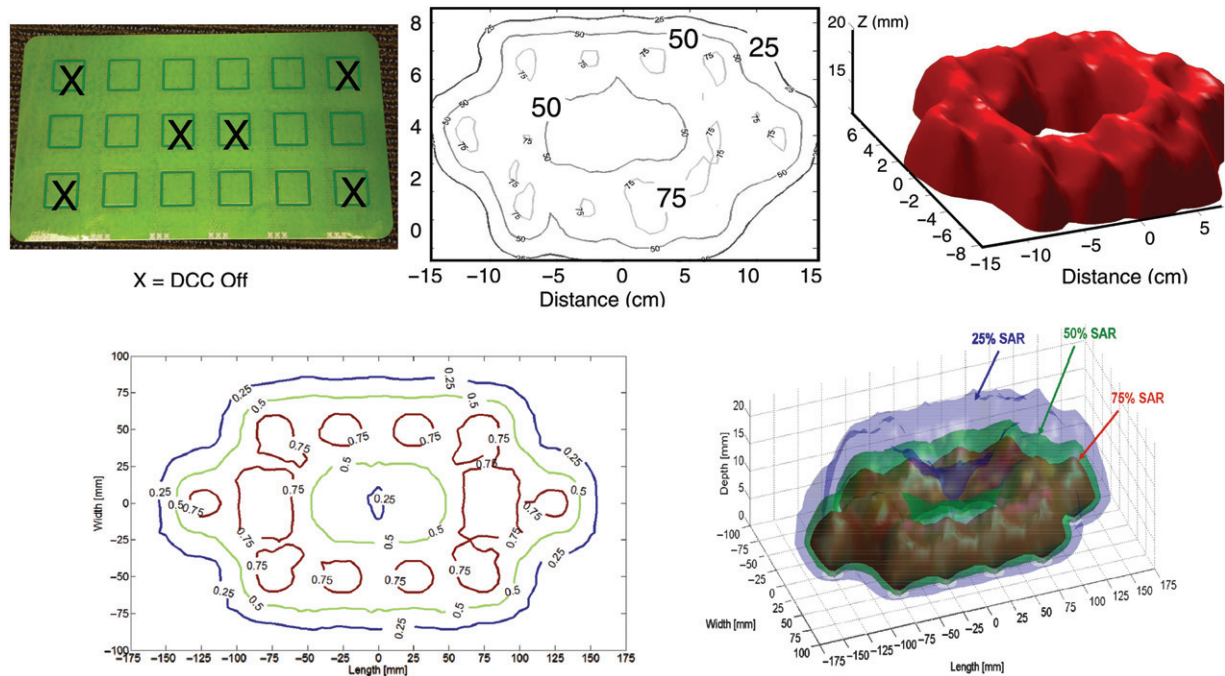


Figure 5. (A) 3×6 DCC array (17×32 cm) fabricated with three-layer LCP and buried coplanar waveguide feed-lines and matching stubs; (B) measured SAR distribution 10 mm deep in muscle-equivalent phantom for the power configuration with six antennas marked with X's turned off; (C) 50% iso-SAR contour in the 10-mm deep plane for the power configuration shown in Figure 5A; (D) HFSS simulated SAR pattern for same power configuration tested in Figure 5B; (E) 3D rendering of HFSS simulation of 25%, 50% and 75% SAR iso-SAR surfaces for same power configuration.

SAR pattern of buried coplanar waveguide CMA

A 3×6 element array of 3 cm square DCC apertures spaced 20 mm apart was fabricated from a 3 layer liquid crystal polymer (LCP) printed circuit board material (Rogers, Chandler, AZ) using a novel double ground layer buried coplanar waveguide feed-line structure. This rectangular DCC array uses the 3 cm^2 radiating slot configuration optimised previously for microstrip DCC arrays and the new feed-line design of the L-shape applicator shown in Figure 2. Figure 5A shows a photo of the 17×32 cm DCC array with Xs marking antennas that are turned off for a demonstration of heating pattern control. Figure 5B shows the SAR pattern measured in a plane 10 mm deep in liquid muscle-equivalent phantom, with no power applied to the four corner elements and two central elements to demonstrate the high degree of conformability to an arbitrary heating configuration. The 50% iso-SAR contour measured in the 10-mm deep plane is shown in Figure 5C for this power configuration. Figures 5D and 5E show the SAR patterns simulated with HFSS for this applicator configuration, for comparison. Note the localisation of power deposition under the powered DCC apertures and effective coverage of heating across large areas of tissue (30–16 cm for this 18 antenna array). The impedance match of this new coplanar waveguide array coupled with a 6 mm water

bolus to muscle-equivalent phantom load was $S_{11} = 10\text{--}12$ db as compared to 6–7 db for earlier microstrip designs. Further improved matching should be achieved with the coplanar arrays coupled to chest wall tissue for which the tuning stubs were designed.

Clinical evaluation of CMA

A clinical evaluation of heating uniformity from CMA applicators was carried out at the University of California San Francisco (UCSF) an IRB approved protocol for microwave array hyperthermia combined with external beam radiation for chest wall recurrence. Thirteen patients signed an informed consent and received one or more 60-min heat treatments using 915 MHz conformal microwave array (CMA) heat applicators ranging in size from 15 to 27 aperture arrays of 3 or 4 cm square DCC apertures. The potential effective treatment area of the CMA applicators was $375\text{--}500 \text{ cm}^2$ along the contoured anatomy surface. Most patients also received heat treatments with a 4×4 planar array microwave system (Microtherm) with approximately 13×13 cm (169 cm^2) treatment area which was the current clinical hyperthermia system for chest wall disease at the time of this investigation. For both systems, temperatures were measured with fibre-optic sensors scanned inside 3–7 catheters crossing the tissue surface as exemplified in the left

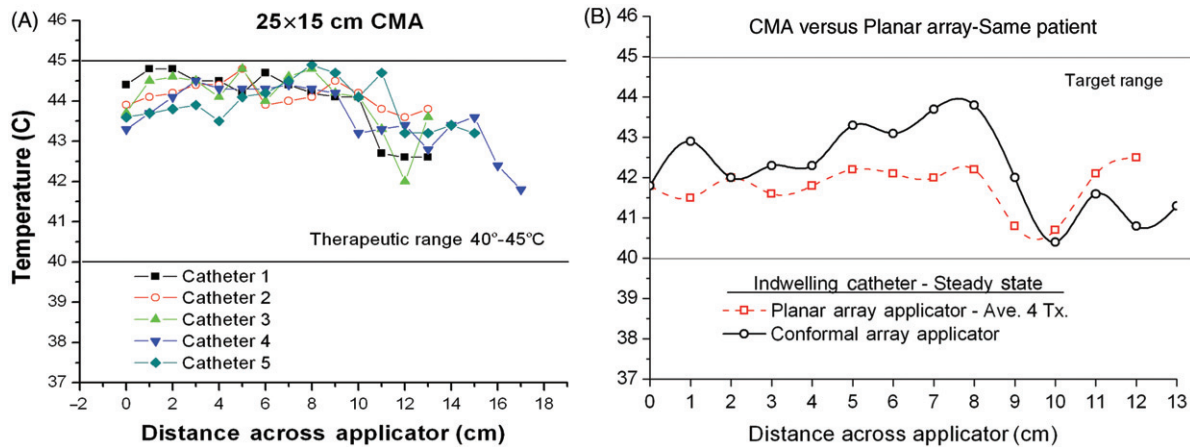


Figure 6. Temperatures measured during clinical hyperthermia with 31×14 cm CMA applicator on a chest wall patient. (A) Temperatures measured at 10 mm increments in four catheters on the tumour target surface and one catheter implanted approximately 10 mm deep, prior to adjusting DCC power levels for most uniform heating. (B) Temperatures measured at 10 mm increments along an indwelling catheter 5–10 mm deep in tissue midway through heat treatments of the same patient, once with a 24 aperture conformal array and average of four successive treatments with a 16 element planar array applicator.

panel of Figure 1, and in some patients also at 10 mm increments along an interstitial catheter that was inserted up to 14 cm at a depth of 5–10 mm beneath the skin. The goals of this initial clinical evaluation of CMA applicator performance were to: (1) demonstrate the ability to heat increasingly larger superficial disease regions over contoured anatomy than possible with previous microwave applicators, (2) characterise uniformity of heating of the selected target region under the conformal array, aiming for therapeutic temperatures in the range of 40°–45°C; (3) produce high thermal dose uniformly within large target regions with acceptable toxicity, demonstrating cumulative thermal doses of $CEM43T_{90} > 10$ equivalent minutes for each treatment, and $CEM43T_{90} > 100$ total for the treatment course of 8–10 treatments, using the thermal dose calculation defined by Dewey [74] and (4) document patient comfort and tolerance to CMA treatments.

Prototype CMA applicators were used for 42 hyperthermia treatments in 13 ethnically diverse female patients with chest wall recurrence, including 7 white, 2 black, 2 Hispanic-Latino, and 2 Asian-Pacific patients. For the evaluation of heating performance of the conformal applicator, tumour target was defined as the extent of visible/palpable disease that fell within the perimeter of the DCC aperture array plus a 10-mm margin. For the 42 heat treatments, the mean number of measured temperature points within the target volume was 90 ± 29 , ranging from 24 to 140 points. In every treatment an attempt was made to distribute thermal mapping catheters evenly across the tissue surface and under each independently powered aperture, and to record temperatures at 10–20 mm increments along each

catheter. Due to the time required for manual mapping of large contoured areas of the torso, complete thermal maps were recorded within the first 15 min of the heat treatment and 1–2 more times during the 60 min treatment. Power levels of individual apertures were balanced based on the thermal maps to produce more uniform temperatures under the array. For this evaluation of applicator heating uniformity, temperatures are generally taken from the second thermal map which is intended to represent the steady state 'adjusted' heating pattern. The mean temperatures measured within the tumour target in these 42 treatments were $T_{\min} = 41.4 \pm 0.7^\circ\text{C}$, $T_{90} = 42.1 \pm 0.6^\circ\text{C}$, $T_{\text{ave}} = 42.8 \pm 0.6^\circ\text{C}$, and $T_{\max} = 44.3 \pm 0.8^\circ\text{C}$. The mean cumulative equivalent minutes thermal dose was $CEM43T_{90} = 23.2 \pm 19.6$ min per treatment. Figure 6A shows a typical recording of mid-treatment thermal dosimetry for a single heat treatment with large 24 element CMA. Temperatures are shown at 10-mm increments along four catheters crossing the tumour target surface under the four rows of six DCC heat apertures. A fifth sensor was thermally mapped at 10-mm increments along an implanted catheter crossing the tumour at approximately 10 mm depth under the applicator. A water bolus temperature of 42°–42.5°C was used as previous clinical experience with both planar and conformal microwave array applicators demonstrated most balanced heating from skin surface to depths of 10–15 mm at this bolus temperature. This observation has subsequently been confirmed with comprehensive thermal modelling [35] that describes somewhat deeper heating to 20 mm depth with cooler bolus and

Table I. Same site thermal dosimetry comparison of the best treatments with conformal microwave array (CMA) and planar array (PA) applicators. Negative values mean the planar array produced higher average temperatures for the measured points in target. Total number of measured points in tumour target is higher for CMA, proportionate to the increased treatment area. Note the planar array was limited to treating a portion (169 cm²) of the disease target whereas the CMA coverage ranged from 288 to 500 cm² as needed to cover the entire tumour target.

Patient #	T_{\max}		T_{\min}		T_{90}		T_{ave}		CEM43 T_{90}		CMA Target	CMA/PA Area Ratio
	CMA	CMA-PA	CMA	CMA-PA	CMA	CMA-PA	CMA	CMA-PA	CMA	CMA-PA		
1	45	1	41.1	0.4	42.2	0.1	42.3	-0.8	20	5	31 × 14	2.6
2	44.4	0.4	42.3	0.7	42.4	0.4	43	0	26	12	22 × 17	2.2
3	43.2	-1.9	41.5	0.2	42.2	0.3	42.5	-0.4	20	7	24 × 12	1.7
4	47	3.8	41.8	0.1	42.5	0.5	43	0.6	30	15	23 × 19	2.6
5	43.9	-0.1	41.3	-0.2	41.9	-0.2	42.4	-0.2	14	-3	25 × 20	3.0
6	43.2	-0.8	41.2	0.1	41.6	-0.3	42	-0.6	8	-4	25 × 20	3.0
7	44.1	0.1	42.1	0.5	42.3	0.1	43.1	0	23	14	25 × 15	2.2

balanced heating from skin to 15 mm depth with 42°C bolus. Although antenna power levels were adjusted based primarily on thermally mapped surface sensors for all patients, some of the treatments had an interstitial catheter to provide 10–15 temperatures at depth in tumour for correlation of surface and deep temperatures. Figure 6B compares heating distributions obtained near mid-treatment in an interstitial catheter 5–10 mm deep in tumour target for two different heat applicators. The dashed curve represents the average interstitial temperatures obtained in four successive treatments with the Microtherm planar array applicator and the solid line data is from a treatment of the same disease with a 24 aperture conformal microwave array. The data show that in this patient, who is typical of other chest wall recurrence cases, the CMA applicator reached higher temperatures in many but not all portions of the tumour target, most likely due to better conformal fit of the heating antennas to the contoured surface. Direct comparison of heating uniformity within the perimeter of each applicator was possible in seven patients treated with both a conformal array and the Microtherm planar array. Table I compares dosimetry parameters for the best treatment obtained with the planar array and CMA applicators treating the same disease in seven patients. Note that the number of measured points and overall treatment volume was higher for the CMA applicators than for the planar array which was limited to 13 × 13 cm effective treatment area. Overall, the CMA applicators produced similarly effective therapeutic heating of large volume disease to the desired 41.5°–44.5°C target range, and in most cases produced higher minimum temperatures and cumulative thermal dose over much larger target areas than possible with the waveguide array.

In addition to the quantitative thermal dosimetry summarised above, the CMA applicators were evaluated in terms of two subjective criteria, including operator friendliness and comments regarding

relative comfort and tolerance to treatment from all patients that were treated with both the planar array and CMA applicator. Since the CMA ranged from 1.7 to 3 times larger effective treatment area than the waveguide array, the entire disease target was generally covered with a single CMA heat treatment, whereas multiple patch area treatments were required to cover the entire disease with the smaller 15 × 15 cm waveguide array. Thus thermal mapping of larger surface areas was required for each CMA treatment, with a correspondingly larger number of measurement points and time for set-up and mapping. Along with placement of the outer elastic support garment to secure the applicator to patient disease, the CMA required approximately 10 min longer for each set-up. For many patients, this extra set-up time was more than compensated by combining multiple 60-min patch treatments into one large area CMA treatment. While the large number of independently controlled power amplifiers required increased thermal mapping activity and translation to power adjustments during treatment, in general the operator appreciated the ability to electronically adjust heating with high resolution to accommodate patient disease on the curving surface of the torso. So in general, the CMA required increased effort on the part of the operator during the 1 h treatment but saved time overall when multiple patch treatments could be accommodated in one large treatment field, and was more responsive to control signals to adjust power for uniform heating.

Although toxicity was not a primary end-point of this thermal dosimetry protocol, there was no unexpected toxicity from use of the CMA applicator nor noticeable difference compared to the 915 MHz planar array which was the standard hyperthermia applicator used at UCSF for chest wall recurrence at the time of this evaluation. Toxicity from use of these 915 MHz hyperthermia applicators in combination with external beam radiotherapy was limited to 10% incidence of minor thermal blisters of previously

irradiated skin, all of which healed without need for medical attention. This is consistent with the toxicities reported in the literature for treatment of previously irradiated chest wall disease with combination heat and radiation [7].

The conformal applicators included a large area thin layer water bolus preheated to 42.5°C that was wrapped over and around the target disease prior to placement of the flexible PCB microwave array. The entire multilayer assembly was covered by an elastic strap or stretch shirt to hold the applicator snugly in place over the tissue target. Comments from all 13 patients documented that they preferred the relative comfort of the snug body conforming applicator compared to the heavy and bulky planar waveguide array which had a floppy water bolus at the same temperature but pressed hard against the skin to ensure skin contact around the periphery of the array. The net effect was that the lightweight conformal array held to the patient surface with an elastic support was notably more comfortable and tolerable for the hour long treatment than the heavy waveguide array which some patients likened to an 'elephant's foot'. In addition, the elastic fixation of applicator over the contoured surface allowed a large range of motion for the patient, whereas the planar array was supported by a holding arm that was fixed in position and thus did not allow patient movement during treatment. In fact, some patients changed positions from lying down to sitting or even standing temporarily while the CMA heating progressed uninterrupted. This ability to move during hyperthermia treatment was a significant factor in the improved comfort and tolerance of patients to the hyperthermia procedure relative to the planar waveguide array applicator. Even when the heated area covered disease up to three times the maximum area treatable with the planar array, patients tolerated the treatments better and with higher overall treatment temperatures.

Conclusion

Recurrent breast cancer patients present with a wide range of size, shape and depth of disease. The literature is rife with examples of how heat can be used to enhance therapeutic results of radiation and chemotherapy, but previous clinical results have been obtained with less than optimal hyperthermia equipment that often limits the quality and extent of heating, and ease of application. This has reduced enthusiasm for thermotherapy even though the results have proven useful when heating is possible. Moving forward, there are a number of devices now available to treat breast and chest wall disease and an increasing number of devices in final stages of

development for accommodating a larger number of patients with difficult to heat disease. This article provides an overview of current state of the art in heat applicators and temperature measurement approaches for diffuse superficial chest wall disease, with emphasis on a device intended to treat the largest area disease extending beyond the anterior chest wall. This CMA applicator may be configured as a conformal wrap around the anterior and lateral chest, or expanded into a complete vest to treat diffuse disease extending across the torso. An evaluation of heating performance of large conformal microwave array applicators with up to 500 cm² treatment area is presented. First the power deposition pattern is given for a large multiaperture DCC array coupled to a homogeneous muscle tissue-equivalent load to demonstrate the high degree of control of heating within the DCC array constructed from new coplanar waveguide feed-line network. Next the power deposition pattern is calculated for a typically contoured patient and superimposed on a realistic contoured anatomy as obtained from an MR scan of a single mastectomy patient. Most importantly, CMA applicator heating performance is evaluated in a small pilot study in 13 patients heated with both a 4 × 4 planar waveguide array and a CMA applicator. Direct quantitative comparison of thermal dosimetry is presented for seven patients in which the same disease site was treated with matching thermal mapping and qualitative comparison of relative patient comfort and tumour coverage is given for all 13 patients. The results demonstrate similarly therapeutic heating to the intended 41.5°–44.5°C range within the perimeter of the heat applicators for both microwave array applicators with a minor increase in minimum and average temperatures achieved with the conformal array. In addition the conformal arrays were able to treat a larger effective area over contoured regions of the anatomy that required multiple placements of the smaller planar array applicator. Overall, the prototype conformal array applicators provided well-tolerated heating within the desired range, with temperature parameters of $T_{\min} = 41.4 \pm 0.7^\circ\text{C}$, $T_{90} = 42.1 \pm 0.6^\circ\text{C}$, $T_{\text{ave}} = 42.8 \pm 0.6^\circ\text{C}$, and $T_{\max} = 44.3 \pm 0.8^\circ\text{C}$ obtained in an average of 90 measured points per treatment. The CMA applicator appears to be an effective hyperthermia device to treat large area superficial disease such as diffuse chest wall recurrence of breast cancer.

Acknowledgements

The authors would like to acknowledge substantial contributions to the CMA applicator design and testing from previous active collaborators including

Daniel Neuman, David Bozzo, Vinicio Manfrini, Svein Jacobsen and Yngve Birkelund.

Declaration of interest: The authors would like to acknowledge NIH support of CMA applicator development which has evolved from work on NIH Grants RO1-CA70761, R43-CA69868, R43-AR51278, R43/44-RR14940, R43/44-CA104061, and PO1-CA42745. In addition, the authors would like to recognise important contributions from a number of corporate collaborators, including simulation software and technical support from Dane Thompson and Ansys/Ansoft, power system from Ron Johnston at Labthermics Technologies, fibre-optic thermal monitoring sheet from Celestino Gaeta at Iptek, radiometric monitoring system from Fred Sterzer at MMTC, and water bolus and patient interface developments from Bionix Development. The authors alone are responsible for the content and writing of the paper.

References

1. Cancer Facts and Figures 2009-2010: American Cancer Society, 2009.
2. Kleer CG, van, Golen KL, Merajver SD. Molecular biology of breast cancer metastasis. Inflammatory breast cancer: Clinical syndrome and molecular determinants. *Breast Cancer Res* 2000;2:423-429.
3. Donegan W, Perez-Mesa C, Watson F. A biostatistical study of local recurrent breast cancer. *Surg Gynecol Obstet* 1966;122:529-540.
4. Henderson I, Harris J, Kinne D, Hellman S. Cancer of the breast. In: DeVita VJ, Hellman S, and Rosenberg S, editors. *Cancer: Principles and Practice of Oncology*, 3rd edn. Philadelphia: JB Lippincott; 1989. pp 1197-1249.
5. Kapp DS. Efficacy of adjuvant hyperthermia in the treatment of superficial recurrent breast cancer: Confirmation and future directions. *Int J Radiat Oncol Biol Phys* 1996;35:1117-1121.
6. Seegenschmiedt MH, Fessenden P, Vernon CC. *Thermoradiotherapy and Thermochemotherapy. Clinical Applications. Vol. 2.* Berlin, New York: Springer Verlag; 1996.
7. Sneed PK, Stauffer PR, Li GC. Hyperthermia. In: Leibel SA and Phillips TL, editors. *Textbook of Radiation Oncology*, 2nd edn. Philadelphia: WB Saunders; 2004. pp 1569-1596.
8. Dewhirst MW, Jones E, Samulski TV, Vujaskovic Z, Li C, Prosnitz L, Hyperthermia.. In: Kufe D, Pollock R, Weischelbaum R, Gansler RBT, Holland J, and FRei E, editors. *Cancer Medicine*, 6th edn. Hamilton, BC, Canada: Decker; 2003. pp 623-636.
9. Jones EL, Oleson JR, Prosnitz LR, Samulski TV, Vujaskovic Z, Yu D, Sanders LL, Dewhirst MW. Randomized trial of hyperthermia and radiation for superficial tumors. *J Clin Onc* 2005;23:3079-3085.
10. Vernon CC, Hand JW, Field SB, Machin D, Whaley JB, van der Zee J, van Putten WLJ, van Rhooen GC, van Dijk JDP, Gonzalez-Gonzalez D, et al. Radiotherapy with or without hyperthermia in the treatment of superficial localized breast cancer: Results from five randomized controlled trials. *Int J Radiat Oncol Biol Phys* 1996;35:731-744.
11. Hand JW, Machin D, Vernon CC, Whaley JB. Analysis of thermal parameters obtained during phase III trials of hyperthermia as an adjunct to radiotherapy in the treatment of breast carcinoma. *Int J Hyperthermia* 1997;13:343-364.
12. Stauffer PR. Thermal therapy techniques for skin and superficial tissue disease. In: Ryan TP, editor. *A critical review, matching the energy source to the clinical need.* Bellingham WA: SPIE Optical Engineering Press; 2000. pp. 327-367.
13. Lee ER. *Electromagnetic Superficial Heating Technology.* In: Seegenschmiedt MH, Fessenden P, Vernon CC, editors. *Thermoradiotherapy and Thermochemotherapy.* Berlin, Heidelberg: Springer-Verlag; 1995. pp. 193-217.
14. Stauffer PR, Diederich CJ, Pouliot J. Thermal therapy for cancer. In: Thomadsen B, Rivard M, Butler W, editors. *Brachytherapy Physics, second edition, Joint AAPM/ABS Summer School, Med Phys Monograph No 312005.* Madison, WI: Medical Physics Publishing, pp 901-932; 2005.
15. Hynynen K, Roemer R, Anhalt D, Johnson C, Xu ZX, Swindell W, Cetas TC. A scanned, focused, multiple transducer ultrasonic system for localized hyperthermia treatments. *Int J Hyperthermia* 2010;26:1-11.
16. Penagaricano JA, Moros E, Novak P, Yan Y, Corry P. Feasibility of concurrent treatment with the scanning ultrasound reflector linear array system (SURLAS) and the helical tomotherapy system. *Int J Hyperthermia* 2008;24:377-388.
17. Novak P, Moros EG, Straube WL, Myerson RJ. SURLAS: A new clinical grade ultrasound system for sequential or concomitant thermoradiotherapy of superficial tumors: Applicator description. *Med Phys* 2005;32:230-240.
18. Diederich CJ, Stauffer PR. Pre-clinical evaluation of a microwave planar array applicator for superficial hyperthermia. *Int J Hyperthermia* 1993;9:227-246.
19. Johnson JE, Neuman DG, Maccarini PF, Juang T, Stauffer PR, Turner P. Evaluation of a dual-arm Archimedean spiral array for microwave hyperthermia. *Int J Hyperthermia* 2006;22:475-490.
20. Lee ER, Wilsey TR, Tarczy-Hornoch P, Kapp DS, Fessenden P, Lohrbach AW, Prionas SD. Body conformable 915 MHz microstrip array applicators for large surface area hyperthermia. *IEEE Trans Biomed Eng* 1992;39:470-483.
21. Gelvich EA, Mazokhin VN. Contact flexible microstrip applicators (CFMA) in a range from microwaves up to short waves. *IEEE Trans Biomed Eng* 2002;49:1015-1023.
22. Lamaitre G, Van Dijk JDP, Gelvich EA, Wiersma J, Schneider CJ. SAR characteristics of three types of contact flexible microstrip applicators for superficial hyperthermia. *Int J Hyperthermia* 1996;12:255-269.
23. Kok HP, Correia D, De, Greef M, Van Stam G, Bel A, Crezee J. SAR deposition by curved CFMA-434 applicators for superficial hyperthermia: Measurements and simulations. *Int J Hyperthermia* 2010;26:171-184.
24. Rossetto F, Stauffer PR, Manfrini V, Diederich CJ, Gentili Biffi, G. Effect of practical layered dielectric loads on SAR patterns from dual concentric conductor microstrip antennas. *Int J Hyperthermia* 1998;14:513-534.
25. Rossetto F, Stauffer PR. Effect of complex bolus-tissue load configurations on SAR distributions from dual concentric conductor applicators. *IEEE Trans Biomed Eng* 1999;46:1310-1319.
26. Rossetto F, Diederich CJ, Stauffer PR. Thermal and SAR characterization of multielement dual concentric conductor microwave applicators for hyperthermia, a theoretical investigation. *Med Phys* 2000;27:745-753.
27. Rossetto F, Stauffer PR. Theoretical characterization of dual concentric conductor microwave array applicators for

- hyperthermia at 433 MHz. *Int J Hyperthermia* 2001;17(3): 258–270.
28. Stauffer PR, Leoncini M, Manfrini V, Gentili GB, Diederich CJ, Bozzo D. Dual concentric conductor radiator for microwave hyperthermia with improved field uniformity to periphery of aperture. *IEICE Trans on Communicat* 1995; E78-B(6):826–835.
 29. Stauffer PR, Rossetto F, Leoncini M, Gentili GB. Radiation patterns of dual concentric conductor microstrip antennas for superficial hyperthermia. *IEEE Trans Biomed Eng* 1998;45:605–613.
 30. Stauffer PR, Jacobsen S, Neuman D. Microwave array applicator for radiometry controlled superficial hyperthermia. In: Ryan TP, editor. *Thermal Treatment of Tissue: Energy Delivery and Assessment*. San Jose: Proc SPIE, 2001, pp 19–29.
 31. Stauffer P, Maccarini P, Juang T, Jacobsen S, Gaeta C, Schlorff J, Milligan A. Progress on conformal microwave array applicators for heating chest wall disease. In: Ryan T, editor. *Proc SPIE*. Vol. 6440. Bellingham, WA: SPIE Press; 2007. pp OE-1–13.
 32. Stauffer P, Schlorff J, Taschereau R, Juang T, Neuman D, Maccarini P, Pouliot J, Hsu J. Combination applicator for simultaneous heat and radiation. *Conf Proc IEEE Eng Med Biol Soc* 2004;4:2514–2517.
 33. Stauffer PR, Schlorff JL, Juang T, Neuman DG, Johnson JE, Maccarini PF, Pouliot J, editors. Progress on system for applying simultaneous heat and brachytherapy to large-area surface disease. In: Ryan TP, editor. *SPIE BiOS 2005*. San Jose: SPIE Press; 2005.
 34. Arunachalam K, Craciunescu O, Maccarini P, Schlorff J, Markowitz E, Stauffer P, editors. Progress on thermobrachytherapy surface applicator for superficial tissue diseases. *Proc SPIE*. Bellingham, WA: SPIE Press, 2009.
 35. Arunachalam K, Maccarini P, Craciunescu O, Schlorff J, Stauffer P. Thermal characteristics of thermobrachytherapy surface applicators (TBSA) for treating chest wall recurrence. *Phys Med Biol* 2010;55:1949–1969.
 36. Chan KW, Chou CK. Use of the thermocouples in the intense fields of ferromagnetic implant hyperthermia. *Int J Hyperthermia* 1993;9:831–848.
 37. Chan KW, Chou CK, McDougall JA, Luk KH. Changes in heating patterns due to perturbations by thermometer probes at 915 and 434 MHz. *Int J Hyperthermia* 1988;4: 447–456.
 38. Bowman R. A probe for measuring temperature in radio-frequency heated material. *IEEE Trans Mic Theory Tech* 1976;24:43–45.
 39. Chan KW, Chou CK, McDougall JA, Luk KH. Perturbations due to the use of catheters with non-perturbing probes. *Int J Hyperthermia* 1988;4:699–702.
 40. Cetas TC. Practical thermometry with a thermographic camera – Calibration, transmittance, and emittance measurements. *Rev Sci Instrum* 1978;49:245–254.
 41. Arunachalam K, Maccarini P, Juang T, Gaeta C, Stauffer PR. Performance evaluation of a conformal thermal monitoring sheet sensor array for measurement of surface temperature distributions during superficial hyperthermia treatments. *Int J Hyperthermia* 2008;24:313–325.
 42. Arunachalam K, Maccarini PF, Stauffer PR. A thermal monitoring sheet with low influence from adjacent waterbolus for tissue surface thermometry during clinical hyperthermia. *IEEE Trans Biomed Eng* 2008;55:2397–2406.
 43. Bardati F, Brown VJ, Tognolatti P. Temperature reconstructions in a dielectric cylinder by multi-frequency microwave radiometry. *J Electromagnet Wave Appl* 1993;7:1549–1571.
 44. Hand JW, Van Leeuwen GMJ, Mizushima S, Van De Kamer JB, Maruyama K, Sugiura T, Azzopardi DV, Edwards AD. Monitoring of deep brain temperature in infants using multi-frequency microwave radiometry and thermal modelling. *Phys Med Biol* 2001;46:1885–1903.
 45. Jacobsen S, Stauffer P. Multi-frequency radiometric determination of temperature profiles in a lossy homogenous phantom using a dual-mode antenna with integral water bolus. *IEEE Trans Mic Theory Tech* 2002;50:1737–1746.
 46. Jacobsen S, Stauffer P. Non-invasive temperature profile estimation in a lossy medium based on multi-band radiometric signals sensed by a microwave dual-purpose body-contacting antenna. *Int J Hyperthermia* 2002;18(2): 86–103.
 47. Mizushima S, Shimizu T, Suzuki K, Kinomura M, Ohba H, Sugiura T. Retrieval of temperature-depth profiles in biological objects from multi-frequency microwave radiometric data. *J Electromagnet Wave Appl* 1993;7:1515–1548.
 48. Camart JC, Despretz D, Prevost B, Sozanski JP, Chive M, Pribetich J. New 434 MHz interstitial hyperthermia system monitored by microwave radiometry: Theoretical and experimental results. *Int J Hyperthermia* 2000;16:95–111.
 49. Fabre JJ, Chive M, Dubois L, Camart JC, Playez E, Prevost B, Vanseymortier L, Rohart J. 915 MHz microwave interstitial hyperthermia. Part I: Theoretical and experimental aspects with temperature control by multifrequency radiometry. *Int J Hyperthermia* 1993;9:433–444.
 50. Chive M, Plancot M, Giaux G, Prevost B. Microwave hyperthermia controlled by microwave radiometry: Technical aspects and first clinical results. *J Microwave Power* 1984;19:233–241.
 51. Jacobsen S, Stauffer PR, Neuman DG. Dual-mode antenna design for microwave heating and noninvasive thermometry of superficial tissue disease. *IEEE Trans Biomed Eng* 2000;47:1500–1509.
 52. Jacobsen S, Stauffer PR. Can we settle with single-band radiometric temperature monitoring during hyperthermia treatment of chest wall recurrence of breast cancer using a dual-mode transceiving applicator? *Physics Med Biol* 2007;21(52):911–928.
 53. Wyatt C, Soher B, Maccarini P, Charles HC, Stauffer P, Macfall J. Hyperthermia MRI temperature measurement: Evaluation of measurement stabilisation strategies for extremity and breast tumours. *Int J Hyperthermia* 2009;25: 422–433.
 54. Carter DL, MacFall JR, Clegg ST, Xin W, Prescott DM, Charles HC, Samulski TV. Magnetic resonance thermometry during hyperthermia for human high-grade sarcoma. *Int J Radiat Oncol Biol Phys* 1998;40:815–822.
 55. Hynynen K, McDannold N. MRI guided and monitored focused ultrasound thermal ablation methods: A review of progress. *Int J Hyperthermia* 2004;20:725–737.
 56. McDannold N, Hynynen K. Quality assurance and system stability of a clinical MRI-guided focused ultrasound system: Four-year experience. *Med Phys* 2006;33:4307–4313.
 57. Samulski TV, MacFall J, Zhang Y, Grant W, Charles C. Non-invasive thermometry using magnetic resonance diffusion imaging: Potential for application in hyperthermic oncology. *Int J Hyperthermia* 1992;8:819–829.
 58. Craciunescu O, Stauffer P, Soher B, Maccarini P, Das S, Cheng K, Stakhursky V, Wyatt C, Wong T, Jones EL, et al. Accuracy of real time noninvasive temperature measurements using magnetic resonance thermal imaging in patients treated for high grade extremity soft tissue sarcomas. *Med Phys* 2009;36(11):4848–4858.
 59. Gellermann J, Włodarczyk W, Feussner A, Fahling H, Nadobny J, Hildebrandt B, et al. Methods and potentials of magnetic resonance imaging for monitoring radiofrequency hyperthermia in a hybrid system. *Int J Hyperthermia*;21: 497–513.

60. Gellermann J, Hildebrandt B, Issels R, Ganter H, Wlodarczyk W, Budach V, et al. Noninvasive magnetic resonance thermography of soft tissue sarcomas during regional hyperthermia: Correlation with response and direct thermometry. *Cancer* 2006;107:1373–1382.
61. McDannold N. Quantitative MRI-based temperature mapping based on the proton resonant frequency shift: Review of validation studies. *Int J Hyperthermia* 2005;21:533–546.
62. Rossetto F, Stauffer PR. Theoretical characterization of dual concentric conductor microwave applicators for hyperthermia at 433MHz. *Int J Hyperthermia* 2001;17:258–270.
63. Maccarini PF, Rolfsnes HO, Neuman D, Stauffer P. Optimization of a dual concentric conductor antenna for superficial hyperthermia applications. *Conf Proc IEEE Eng Med Biol Soc* 2004;4:2518–2521.
64. Maccarini PF, Rolfsnes HO, Johnson J, Neuman DG, Jacobsen S, Stauffer PR. Electromagnetic optimization of dual mode antennas for radiometry controlled heating of superficial tissue. *Proc SPIE*. San Jose: SPIE Press; 2005.
65. Maccarini P, Rolfsnes Jr HO, DGN, Johnson JE, Juang T, Stauffer PR. *IEEE Mic Theory and Tech Society. Advances in microwave hyperthermia of large superficial tumors*. Piscataway NJ: IEEE Press; 2005.
66. Maccarini P, Arunachalam K, Martins C, Stauffer P. Size reduction and radiation pattern shaping of conformal microwave array hyperthermia applicators using multi-fed DCC slot antennas. *Proc SPIE*. Bellingham, WA: SPIE Press; 2009.
67. Juang T, Stauffer PR, Neuman DG, Schlorff JL. Multilayer conformal applicator for microwave heating and brachytherapy treatment of superficial tissue disease. *Int J Hyperthermia* 2006;22:527–544.
68. Arunachalam K, Maccarini PF, Schlorff JL, Birkelund Y, Jacobsen S, Stauffer PR. Design of a water coupling bolus with improved flow distribution for multi-element superficial hyperthermia applicators. *Int J Hyperthermia* 2009;25:554–565.
69. Jacobsen S, Stauffer PR. Can we settle with single-band radiometric temperature monitoring during hyperthermia treatment of chestwall recurrence of breast cancer using a dual-mode transceiving applicator? *Physics in Medicine and Biology* 2007;52(4):911–928.
70. Stauffer PR, Jacobsen S, Neuman D, Rossetto F. *Progress Toward Radiometry Controlled Conformal Microwave Array Hyperthermia Applicator*. Chicago: IEEE Engineering in Medicine and Biology Society, 2000.
71. Stauffer PR. Evolving technology for thermal therapy of cancer. *Int J Hyperthermia* 2005;21:731–744.
72. Birkelund Y, Jacobsen S, Arunachalam K, Maccarini P, Stauffer PR. Flow patterns and heat convection in a rectangular water bolus for use in superficial hyperthermia. *Phys Med Biol* 2009;54:3937–3953.
73. Dewey WC. Arrhenius relationships from the molecule and cell to the clinic. *Int J Hyperthermia* 1994;10:457–483.